International Tables for Crystallography (2012). Vol. F, Chapter 8.2, pp. 205–210.

Chapter 8.2. Laue crystallography: time-resolved studies

K. Moffat

8.2.1. Introduction

The term 'Laue diffraction' describes the process of X-ray scattering that occurs when a stationary crystal is illuminated by a polychromatic beam of X-rays. The process therefore differs from the now more conventional diffraction techniques in which a moving crystal is illuminated by a monochromatic beam of X-rays. Although Laue diffraction was widely used for structure analysis in the early days of crystallography by Pauling, Bragg, Wyckoff and others, by the 1930s it was superseded by arguably simpler and more readily quantifiable monochromatic techniques. With the advent of naturally polychromatic synchrotron sources in the 1970s, it was natural to (re-)examine the suitability of the Laue technique. The first synchrotron-based Laue experiments to be published appear to have been those of Wood *et al.* (1983) for a small inorganic crystal and of Moffat *et al.* (1984) for a macromolecular crystal; see also Helliwell (1984, 1985). These experimenters realized that the Laue technique afforded exposure times that were short even with respect to those obtainable with similar crystals at the same synchrotron source using conventional monochromatic techniques, and much shorter than those obtainable with laboratory X-ray sources. This advantage, along with the use of a stationary crystal, the large number of Laue spots evident in a single image and the clear distinction of the Laue spots from the underlying X-ray background, suggested that the Laue technique might be particularly applicable to time-resolved crystallography. In this form of crystallography, the total X-ray scattering from the crystal (both the Bragg scattering and the diffuse, non-Bragg scattering) varies with time as the position and/or extent of order of the atoms in the crystal changes in response to some structural perturbation.

It is one thing to propose that a venerable technique may be applicable to a new class of experiments; it is quite another to identify and overcome the complexities and disadvantages of that technique, and to demonstrate how experiments should be conducted and raw data accurately reduced to structure amplitudes. It took roughly 15 years and the efforts of many investigators before it could be stated that Laue crystallography is coming of age (Ren *et al.*, 1999).

The redevelopment of Laue diffraction has depended on three main advances: the use of very intense polychromatic synchrotron sources; the realization that the so-called energy-overlap or overlapping-orders problem in Laue diffraction was theoretically tractable, of limited extent and could be overcome experimentally; and the development of appropriate algorithms and suitable software to address the energy-overlap, spatial-overlap and wavelength-normalization problems. All are discussed below.

Since both Laue crystallography and its applications to time-resolved studies have recently been described at length, this article emphasizes only the key points and directs the reader to the primary and review literature for the details.

8.2.2. Principles of Laue diffraction

The principles of Laue diffraction have been reviewed by Amorós *et al.* (1975), Cruickshank *et al.* (1987, 1991), Helliwell *et al.* (1989), Cassetta *et al.* (1993), Moffat (1997), and Ren *et al.* (1999).

Assume that a stationary, perfect single crystal that diffracts to a resolution limit of d^*_{max} is illuminated by a polychromatic X-ray beam spanning the wavelength (energy) range from λ_{min} (E_{max}) to λ_{max} (E_{min}). All reciprocal-lattice points that lie between the Ewald spheres of radii $1/\lambda_{min}$ and $1/\lambda_{max}$, and within a radius d^*_{max} of the origin O where $d^*_{max} = 1/d_{min}$, the resolution limit of the crystal, are in a diffracting position for a particular wavelength λ, where $\lambda_{min} \leq \lambda \leq \lambda_{max}$ and will contribute to a spot on the Laue diffraction pattern (Fig. 8.2.2.1). All such points diffract simultaneously and throughout the exposure, in contrast to a monochromatic diffraction pattern in which each point diffracts sequentially and briefly as it traverses the Ewald sphere. A Laue pattern may alternatively be thought of as the superposition of a series of monochromatic still patterns, each arising from a different wavelength in the range from λ_{min} to λ_{max}.

Each Laue spot arises from the mapping of a complete ray (a central line in reciprocal space, emanating from the origin) onto a point on the detector. In contrast, each spot in a monochromatic pattern arises from the mapping of a single reciprocal-lattice point onto a point on the detector. A ray may contain only a single reciprocal-lattice point *hkl* with spacing d^*, in which case the corresponding Laue spot arises from a single wavelength (energy) and structure amplitude, or it may contain several

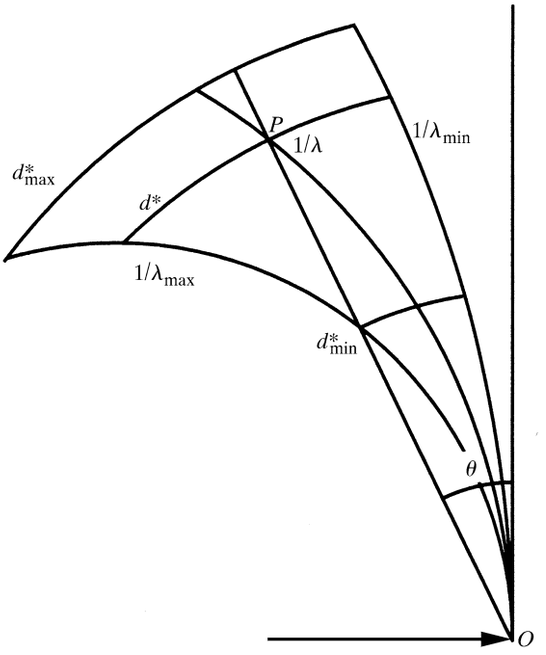

Figure 8.2.2.1
Laue diffraction geometry. The volume element dV stimulated in a Laue experiment lies between d^* and $d^* + \mathrm{d}d^*$, between the Ewald spheres corresponding to λ and $\lambda + \mathrm{d}\lambda$, and between φ and $\varphi + \mathrm{d}\varphi$, where φ denotes rotation about the incident X-ray beam direction. The entire volume stimulated in a single Laue exposure lies between 0 and d^*_{max}, between the Ewald spheres corresponding to λ_{min} and λ_{max}, and between values of θ ranging from 0 to 2π.

reciprocal-lattice points, such as $hkl, 2h2k2l \ldots nhnknl \ldots$, in which case the Laue spot contains several wavelengths (energies) and structure amplitudes. In the former case, the Laue spot is said to be single, and in the latter, multiple. The existence of multiple Laue spots is known as the energy-overlap problem: one spot contains contributions from several energies. It seems to have been thought by Pauling, Bragg and others that, as the wavelength range and the resolution limit $d^*_{\max}$ of the crystal increased, more and more Laue spots would be multiple and the energy-overlap problem would dominate. Cruickshank *et al.* (1987) showed that this was not so. Even in the extreme case of infinite wavelength range, no more than 12.5% of all Laue spots would be multiple. The energy-overlap problem is evidently of restricted extent. However, the magnitude of the energy-overlap problem varies with resolution: reciprocal-lattice points at low resolution are more likely to be associated with multiple Laue spots than to be single (Cruickshank *et al.*, 1987).

The extraction of X-ray structure amplitudes from a single Laue spot requires the derivation and application of a wavelength-dependent correction factor known as the wavelength normalization curve or λ-curve. This curve and other known factors relate the experimentally measured raw intensities of each Laue spot to the square of the corresponding structure amplitude. The integrated intensity of a Laue spot is achieved automatically by integration over wavelength, rather than in a monochromatic spot by integration over angle as the crystal rotates. If, however, a Laue spot is multiple, its total intensity arises from the sum of the integrated intensities of each of its components, known also as harmonics or orders *nhnknl* of the inner point *hkl* where *h*, *k* and *l* are co-prime.

Laue spots lie on conic sections, each corresponding to a central zone [*uvw*] in reciprocal space. Prominent spots known as nodal spots or nodals lie at the intersection of well populated zones and correspond to rays whose inner point *hkl* is of low co-prime indices. All nodal spots are multiple and all are surrounded by clear areas devoid of spots.

The volume of reciprocal space stimulated in a Laue exposure, V_v, is given by

$$V_v = 0.24\ d^{*4}_{\max}(\lambda_{\max} - \lambda_{\min}),$$

and contains N_v reciprocal-lattice points where $N_v = V_v/V^*$ and V^* is the volume of the reciprocal unit cell (Moffat, 1997). N_v can be large, particularly for crystals that diffract to high resolution and thus have larger values of $d^*_{\max}$. Laue patterns may therefore contain numerous closely spaced spots and exhibit a spatial-overlap problem (Cruickshank *et al.*, 1991). The value of N_v is up to an order of magnitude greater than the typical number of spots on a monochromatic oscillation pattern from the same crystal. Since the overall goal of a diffraction experiment is to record all spots in the unique volume of reciprocal space with suitable accuracy and redundancy, a Laue data set may contain fewer images and more spots of higher redundancy than a monochromatic data set (Clifton *et al.*, 1991). This is particularly evident if the crystal is of high symmetry.

Kalman (1979) provided derivations of the integrated intensity of a single spot in the Laue case and in the monochromatic case. Moffat (1997) used these to show that the duration of a typical Laue exposure was between three and four orders of magnitude less than the corresponding monochromatic exposure. The physical reason for this significant Laue advantage lies in the fact that all Laue spots are in a diffracting position and contribute to the integrated intensity throughout the exposure. In contrast, monochromatic spots diffract only briefly as each sweeps through the narrow Ewald sphere [more strictly, through the volume between the closely spaced Ewald spheres corresponding to $1/\lambda$ and $1/(\lambda + d\lambda)$]. The details are modified slightly for mosaic crystals of finite dimensions subjected to an X-ray beam of finite cross section and angular crossfire (Ren *et al.*, 1999; Z. Ren, unpublished results).

Exposure times are governed not merely by the requirement to generate sufficient diffracted intensity in a spot – the signal – but also to minimize the background under the spot – the noise. The background under a Laue spot tends to be higher than under a monochromatic spot, since it arises from a larger volume of reciprocal space in the Laue case. This volume extends from $d^*_{\min}$ (where $d^*_{\min} = 2\sin\theta/\lambda_{\max}$ and θ is the Bragg angle for that Laue spot) through the Laue spot at d^* to either $d^*_{\max}$ or $2\sin\theta/\lambda_{\min}$, whichever is the smaller (Moffat *et al.*, 1989). Since both the signal and the noise in a Laue pattern are directly proportional to the exposure time, their ratio is independent of that parameter. The ratio does depend on the wavelength range $(\lambda_{\max} - \lambda_{\min})$. Decreasing the wavelength range both generates fewer spots and increases the signal-to-noise ratio for each remaining spot by diminishing the background under it. This is analogous to decreasing the oscillation range in a monochromatic exposure.

The choice of appropriate exposure time in the Laue case is complicated, but the central fact remains: both in theory and in practice, Laue exposures are very short with respect to monochromatic exposures (Moffat *et al.*, 1984; Helliwell, 1985; Moffat, 1997). Satisfactory Laue diffraction patterns have been routinely obtained with X-ray exposures of 100 to 150 ps, corresponding to the duration of a single X-ray pulse emitted by a single 15 mA bunch of electrons circulating in the European Synchrotron Radiation Facility (ESRF) (Bourgeois *et al.*, 1996).

The advantages and disadvantages of the Laue technique, compared to the better-established and more familiar monochromatic techniques, are presented in Table 8.2.2.1.

8.2.3. Practical considerations in the Laue technique

The experimental aspects of a Laue experiment – the source and optics, the shutters and other beamline components, detectors, analysis software, and the successful design of the Laue experiments themselves – have been presented by Helliwell *et al.* (1989), Ren & Moffat (1994, 1995*a*,*b*), Bourgeois *et al.* (1996), Ren *et al.* (1996), Clifton *et al.* (1997), Moffat (1997), Yang *et al.* (1998), and Ren *et al.* (1999). Certain key parameters are under the experimenter's control, such as the nature of the source (bending magnet, wiggler or undulator), the wavelength range incident on the crystal (as modified by components of the beamline such as a mirror and attenuators), the choice of detector (active area, number of pixels and the size of each, dependence of detector parameters on wavelength, inherent background, and the accuracy and speed of readout), the experimental data-collection strategy (exposure time or times, number of angular settings of the crystal to be employed and the angular interval between them) and the data-reduction strategy (properties of the algorithms employed and of the software analysis package). A successful Laue experiment demands consideration of these parameters jointly and in advance, as described in these references. The goal is accurate structure amplitudes, not just speedily obtained, beautiful diffraction images.

For example, an undulator source yields a spectrum in which the incident intensity varies sharply with wavelength. Such a source should only be employed if the software can model this

Table 8.2.2.1
Advantages and disadvantages of the Laue technique

This table is adapted from Moffat (1997). See also Ren *et al.* (1999).

Advantages
Shortest possible exposure time, well suited to rapid time-resolved studies that require high time resolution.
Insensitive to all temporal fluctuations in the beam incident on the crystal, whether arising from the source itself, the optical components of the beamline or the shutter train. (Sensitive only to unusual fluctuations of the shape of the incident spectrum with time.)
All spots in a local region of the detector have an identical profile; none are (geometrically) partial.
Requires a stationary crystal and relatively simple optical components, therefore images are easy to acquire.
A large volume of reciprocal space is surveyed per image, hence fewer images are necessary to survey the entire unique volume.
High redundancy of measurements readily obtained, particularly at high resolution.
Disadvantages
Energy overlaps must be deconvoluted into their components if complete data are to be obtained, particularly at low resolution.
Spatial overlaps are numerous, particularly for mosaic crystals, and must be resolved.
Completeness at low resolution may be low, which would lead to significant series-termination errors in Fourier maps.
The rate of heating owing to X-ray absorption can be very high.
The wider the wavelength range, the higher the background under each spot; a trade-off is unavoidable between coverage of reciprocal space and accuracy of intensity measurements.
Spot shape is quite sensitive to crystal disorder.
More complicated wavelength-dependent corrections must be derived and applied to spot intensities to yield structure amplitudes.

variation suitably in the derivation of the wavelength normalization curve. This is indeed so (at least for the *LaueView* software package) even in the most extreme case, that of the so-called single-line undulator source in which λ_{max} and λ_{min} may differ by only 10%, say by 0.1 Å at 1.0 Å (V. Šrajer *et al.* and D. Bourgeois *et al.*, in preparation).

As a second example, a Laue diffraction pattern is particularly sensitive to crystal disorder, which leads to substantial 'streaking' of the Laue spots that is predominantly radial in direction in each diffraction image and may be dependent both on direction in reciprocal space (anisotropic disorder) and on time (if, in a time-resolved experiment, disorder is induced by the process of reaction initiation or by structural evolution as the reaction proceeds). The software therefore has to be able to model accurately elongated closely spaced or partially overlapping spots, whose profile varies markedly with position on each detector image and with time (Ren & Moffat, 1995*a*). If the software has difficulty with this task, then either a more ordered crystal must be selected, thus diminishing the size of each spot and the extent of spatial overlaps, or a narrower wavelength range must be used, thus reducing the total number of spots per image and their average spatial density (Cruickshank *et al.*, 1991); or the crystal-to-detector distance must be increased, thus increasing the average spot-to-spot distance and potentially increasing the signal-to-noise ratio. There are, however, trade-offs. More ordered crystals may not be readily available, a narrower wavelength range means that more images are required for a complete data set and the detector must continue to intercept all of the high-angle diffraction data (which consist largely of single spots stimulated by longer wavelengths).

As a third example, consider radiation damage. This can be purely thermal, arising from heating due to X-ray absorption. The rate of temperature rise may easily reach several hundred kelvin per second from a focused pink bending-magnet beam at second-generation sources such as the National Synchrotron Light Source (NSLS) (Chen, 1994; Moffat, 1997) or several thousand kelvin per second from a focused wiggler source at third-generation sources such as the ESRF. Fast shutters are required to provide an individual exposure of one millisecond or less in the latter case, and hence to limit the temperature rise to a readily survivable value of several kelvin (Bourgeois *et al.*, 1996; Moffat, 1997). Primary radiation damage (arising directly from X-ray absorption and hence from energy deposition) cannot be eliminated, but it may be modified by selection of the wavelength range and by lowering λ_{max}. Secondary radiation damage, arising from the chemical and structural damage generated by highly reactive, rapidly diffusing free radicals, hydrated electrons and other chemical species, can be greatly minimized by the use of very short exposures which allow little time for damaging reactions to occur, and by working at cryogenic temperatures where diffusion is greatly reduced (see *e.g.* Garman & Schneider, 1997). However, the last strategy may not be an option in a time-resolved Laue experiment, where the desired structural transitions may be literally frozen out at cryogenic temperatures.

Extraction of structure amplitudes from a Laue image or data set proceeds through five stages, reviewed in detail by Clifton *et al.* (1997) and Ren *et al.* (1999), and outlined in Fig. 8.2.3.1. First comes the purely geometrical process of indexing, in which each spot is associated with the appropriate *hkl* value and the unit-cell parameters, crystal orientation matrix, λ_{min}, geometric parameters of the detector and X-ray camera, λ_{max} and d^*_{max} are refined, also yielding λ, the wavelength stimulating that spot. In the second stage, each spot is integrated using appropriate profile-fitting algorithms. Thirdly, the wavelength normalization curve is derived, usually by comparison of the recorded intensities of the same (single) spots or symmetry-related spots at several crystal orientations, applied to each image, and the images in each data set scaled together. In the fourth stage, the intensities of spots identified in the first stage as multiple are resolved (or deconvoluted) into the intensity of each individual component or harmonic. The total intensity of a multiple Laue spot is the weighted sum of the intensities of each component, and the weights are known from the wavelength assigned to each component (Stage 1) and the wavelength normalization curve (Stage 3). In the fifth stage, the single and multiple data are merged and reduced to structure amplitudes. Ren *et al.* (1999) have emphasized that, in contrast to the simplified description presented in Section 8.2.2, the effective wavelength range $\lambda_{max} - \lambda_{min}$ depends on resolution, and each Laue spot is stimulated by a range of wavelengths which can be quite large at low resolution. Although typical Laue software packages such as the *Daresbury Laue Software Suite* (Helliwell *et al.*, 1989; Campbell, 1995), *LEAP* (Wakatsuki, 1993) and *LaueView* (Ren & Moffat, 1995*a*,*b*) are largely automated, a surprising degree of manual intervention may still be required in the first (indexing) stage, and in later stages where the order of parameter refine-

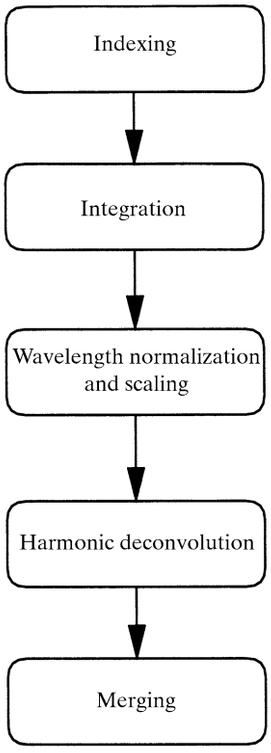

Figure 8.2.3.1
Flow chart of typical Laue data processing.

ment and various rejection criteria may be adjusted by the user. The overall result is that carefully conducted Laue experiments yield structure amplitudes that equal those from monochromatic data in quality (Ren *et al.*, 1999).

8.2.4. The time-resolved experiment

The principles and applications of time-resolved macromolecular crystallography have been widely reviewed (Moffat, 1989; Cruickshank *et al.*, 1992; Hajdu & Johnson, 1993; Helliwell & Rentzepis, 1997; Moffat, 1998; Ren *et al.*, 1999). This article therefore concentrates on the crystallographic aspects.

The essence of a perfect time-resolved crystallographic experiment is that a structural reaction is initiated in all the molecules in the crystal, rapidly, uniformly and in a non-damaging manner. The molecules, far from thermodynamic equilibrium immediately after the completion of the initiation process, relax through a series of structural transitions back to equilibrium. The course of the structural transitions is monitored through the time-dependence of the X-ray scattering. The structure amplitudes (and indeed the phases) associated with each Bragg peak *hkl* become time-dependent and may be denoted $|F(hkl, t)|$. The Fourier transform of the structure factors yields the time-dependent space-average structure of the molecules in the crystal. If all molecules behave independently of one another in the crystal, as they do in dilute solution, then the overall time dependence arises from the time dependence of the fractional populations of each time-independent structural state. That is, the crystal exhibits time-dependent substitutional disorder. (Lest this seem an unfamiliar concept, recall that a multi-site, partially occupied, heavy-atom derivative also exhibits substitutional disorder: the contents of each unit cell differ slightly, depending on whether a particular heavy-atom site is occupied in that unit cell or not. Such disorder fortunately does not invalidate the use of that derivative. The analysis proceeds as though a particular site were, say, 70% occupied in every unit cell of the crystal, although in reality that site is 100% occupied in 70% of the unit cells. In this example, the substitutional disorder is time-independent.) The crystal is thus imperfect: substitutional disorder breaks the translational symmetry. It follows that there must also be time-dependent non-Bragg scattering; but all studies to date have focused on the Bragg scattering.

The above describes a perfect experiment but, as might be expected, reality is different. Initiation techniques such as absorption of light from a laser pulse (Schlichting & Goody, 1997) unavoidably deposit energy in the crystal and give rise to a temperature jump and transient, reversible crystal disorder, evident as spot streaking. The magnitude of this temperature jump is proportional to the number of photons absorbed, which in turn is related to the concentration of photoactive species, the quantum yield for photoactivation and the fraction of molecules stimulated (Moffat, 1995, 1998). The necessity for limiting the magnitude of this temperature jump to retain crystallinity means that it is difficult to initiate the reaction in all molecules in the crystal. For example, photodissociation of carbon monoxide from carbonmonoxymyoglobin crystals was achieved in roughly 40% of the molecules (Šrajer *et al.*, 1996), and entry into the photocycle of photoactive yellow protein in roughly 20% of the molecules (Perman *et al.*, 1998). The magnitude of the time-dependent change in structure-factor amplitudes, given by

$$\Delta F(hkl, t) = |F(hkl, t)| - |F(hkl, 0)|,$$

is proportional to the fraction of molecules photoactivated and is therefore substantially diminished.

The main crystallographic challenge thus becomes the accurate determination of small values of $\Delta F(hkl, t)$ in the face of both random errors (arising from, for example, the small numbers of diffracted photons into the reflection *hkl* from a brief X-ray pulse) and systematic errors (arising from, for example, inaccurate determination of the Laue wavelength normalization curve, crystal-to-crystal scaling errors, inadequately corrected absorption effects, or time-dependent spot profiles). Precision is enhanced by acquiring highly redundant Laue data (mean redundancies typically between 5 and 15), which also afford an excellent measure of the variance of the structure amplitudes, and accuracy is enhanced by interleaving measurements of $|F(hkl, t)|$ with those of $|F(hkl, 0)|$ on the same crystal, at nearly the same time. Indeed, 'two-spot' Laue patterns may be acquired by recording both the $|F(hkl, t)|$ and $|F(hkl, 0)|$ diffraction patterns, slightly displaced with respect to each other, on the same detector [image plate or charge-coupled device (CCD)] prior to readout and quantification (Ren *et al.*, 1996). However, this doubles the background and halves the signal-to-noise ratio.

The values of $\Delta F(hkl, t)$ span a four-dimensional space. What is the best way to scan this four-dimensional space, having regard for the need to minimize errors? Interleaving measurements of $|F(hkl, t)|$ and $|F(hkl, 0)|$ has been achieved by fixing the delay time t between reaction initiation (the pump, laser pulse) and X-ray data acquisition (the probe, X-ray pulse), and surveying all values of *hkl* through progressive reorientation of the crystal between Laue images until all the unique volume of reciprocal space is surveyed with adequate redundancy and completeness (Šrajer *et al.*, 1996; Perman *et al.*, 1998; Ren *et al.*, 1999). The value of t is then altered and data acquisition repeated for all suitable values of t. That is, t is the slow variable. The difficulty with this approach is that a single crystal may yield only one or two data sets, corresponding to one or two values of t, before radiation

damage (predominantly laser-induced rather than X-ray-induced) compels replacement of the crystal. The entire reaction time course over all values of t must therefore be pieced together from measurements on many crystals, a process which is prone to inter-crystal scaling errors. A second experimental approach to scanning this four-dimensional data space is therefore to fix the crystal orientation, obtain values of $|F(hkl, t)|$ and $|F(hkl, 0)|$ for all suitable values of t, reorient the crystal, recollect these same values of t, then replace the crystal and repeat until all the unique volume of reciprocal space is surveyed. That is, hkl are the slow variables (B. Perman, S. Anderson & Z. Ren, unpublished results). This approach yields a more accurate time course, but (for a single crystal) from a subset of reflections only. In practice, of the order of 100 time points t may be collected.

The first approach permits Fourier or difference Fourier maps to be calculated using data from a single crystal at one or a small number of time delays t. The second approach requires data from many crystals to be acquired before such maps can be calculated. This complicates the issue of which is the better approach. Preliminary results (V. Šrajer & B. Perman, unpublished results) suggest that genuine features may be reliably distinguished in real space by examination of Fourier and difference Fourier maps, but genuine trends in reciprocal space are much harder to discern.

How many features can be distinguished as genuine in real space, in, for example, a difference Fourier map? We presently employ three criteria. First, the feature must be 'significant' in crystallographic terms. That is, its peak height must exceed (say) 4σ to 5σ, where σ is the r.m.s. value of the difference electron density $\Delta\rho$ across the asymmetric unit, in a difference Fourier map. Second, the feature must be chemically plausible, *e.g.* located on or near critical groups in the active site. Third, the feature must persist over several time points. No genuine feature is likely to vary faster than exponentially in time (though slower variation is possible), but noise features tend to come and go, varying rapidly with time. The third criterion, which in effect is applying a low-pass temporal filter to the data, or 'time-smoothing', is only applicable if several time points are available per decade of time t. It is to ensure that this powerful criterion can be applied in an unbiased manner that the time points t at which data are acquired are uniformly and closely spaced in log t.

Suppose that complete and accurate values of $|F(hkl, t)|$ are available to high resolution and at numerous values of t. How can these time-dependent data be further analysed to yield information on the reaction mechanism and the time-dependent structures of intermediates? Each candidate chemical-kinetic mechanism implies a different time-dependent mixture of structural states at all times t. For each mechanism, a set of trial time-dependent intermediate structures can be calculated from the time-dependent data (Perman, 1999). One then asks: Is each trial intermediate structure an authentic, single, stereochemically plausible, refinable protein structure? If so, the mechanism is supported, but if not, the mechanism is rejected. This process, of seeking to extract time-independent structures from time-dependent data, is closely related to the better-understood process of extracting time-independent difference spectra from time-dependent optical absorption data *via*, for example, singular value decomposition or principal component analysis. The latter, optical analysis, proceeds in two dimensions, OD(λ, t); the former, crystallographic analysis, must proceed in four dimensions, either $\rho(xyz, t)$ or $|F(hkl, t)|$.

It will be appreciated that the acquisition of fast, time-resolved data is greatly hindered by the lack of a time-slicing area detector. This lack is even more evident when the structural reaction is irreversible as, for example, in the photoactivation of caged GTP to GTP (Schlichting *et al.*, 1990). In such cases, the reactants must be replenished prior to each reaction initiation, which makes the acquisition of time-resolved data particularly tedious. The present generation of CCD detectors have an inter-frame time delay in the millisecond (or just sub-millisecond) time range. Pixel array detectors under development may permit the acquisition of sequential images with a time delay in the microsecond range. The desirable nanosecond or even picosecond time range seems inaccessible for area detectors (but not for point detectors such as streak cameras). A new approach may be needed, such as the use of chirped hard X-ray pulses which, in combination with Laue diffraction, map X-ray energy into both reciprocal space (hkl) and time (K. Moffat, in preparation).

Table 8.2.5.1
Time-resolved Laue diffraction experiments

This table is adapted from Table 2 of Ren *et al.* (1999), in which citations of the original experiments are provided.

Protein	Time resolution	Experiment
Hen lysozyme	64 ms	Temperature jump test
Glycogen phosphorylase	1 s	Bound maltoheptose
Hen lysozyme	1 s	Radiation damage test
Glycogen phosphorylase	100 ms	Use of caged phosphate
Ras oncogene product	1 s	GTP complex
γ-Chymotrypsin	5 s	Photolysis of cinnamate/pyrone
Trypsin	800 ms	Ordered hydrolytic water
Cytochrome *c* peroxidase	1 s	Redox active compound I
Hen lysozyme	10 ms	Temperature jump
Isocitrate dehydrogenase	50 ms	ES complex and intermediate
Isocitrate dehydrogenase	10 ms	Product complex
Photoactive yellow protein	10 ms	*p*B-like intermediate
Photoactive yellow protein	10 ns	*p*R-like intermediate
CO-myoglobin	10 ns	Photolyzed CO species at 290 K
CO-myoglobin	8 ms	Photolyzed CO species at 20–40 K
Hydroxymethylbilane synthase	1.5 ms	Mutant enzyme–cofactor complex

8.2.5. Conclusions

Only a small number of biochemical systems have been subjected to time-resolved crystallographic analysis (Table 8.2.5.1; Ren *et al.*, 1999). The experiments are technically demanding, require careful planning in the execution, in data analysis and in data interpretation, and strategies for the evaluation of mechanism are still being developed. However, road maps exist for several successful classes of experiments (see *e.g.* Stoddard *et al.*, 1998; Moffat, 1998; Ren *et al.*, 1999) and new biological systems to which such analyses may be readily applied are being developed. In a world of structural genomics where structures themselves are ten-a-penny, a structure-based understanding of mechanism at the chemical level is still rare. The contributions of crystallography to functional – not merely structural – genomics may be large indeed.

This work was supported by the NIH. I thank Zhong Ren for comments on the manuscript.

References

Amorós, J. L., Buerger, M. J. & Canut de Amorós, M. (1975). *The Laue Method.* New York: Academic Press.

Bourgeois, D., Ursby, T., Wulff, M., Pradervand, C., Legrand, A., Schildkamp, W., Labouré, S., Srajer, V., Teng, T. Y., Roth, M. & Moffat, K. (1996). *Feasibility and realization of single-pulse Laue diffraction on macromolecular crystals at ESRF. J. Synchrotron Rad.* **3**, 65–74.

Campbell, J. W. (1995). *LAUEGEN, an X-windows-based program for the processing of Laue X-ray diffraction data. J. Appl. Cryst.* **28**, 228–236.

Cassetta, A., Deacon, A., Emmerich, C., Habash, J., Helliwell, J. R., McSweeney, S., Snell, E., Thompson, A. W. & Weisgerber, S. (1993). *The emergence of the synchrotron Laue method for rapid data collection from protein crystals*. *Proc. R. Soc. London Ser. A*, **442**, 177–192.

Chen, Y. (1994). PhD thesis, Cornell University, USA.

Clifton, I. J., Duke, E. M. H., Wakatsuki, S. & Ren, Z. (1997). *Methods Enzymol.* **277**, 448–467.

Clifton, I. J., Elder, M. & Hajdu, J. (1991). *Experimental strategies in Laue crystallography. J. Appl. Cryst.* **24**, 267–277.

Cruickshank, D. W. J., Helliwell, J. R. & Johnson, L. N. (1992). *Time-Resolved Macromolecular Crystallography*. Oxford: Oxford Science Publications.

Cruickshank, D. W. J., Helliwell, J. R. & Moffat, K. (1987). *Multiplicity distribution of reflections in Laue diffraction*. *Acta Cryst.* A**43**, 656–674.

Cruickshank, D. W. J., Helliwell, J. R. & Moffat, K. (1991). *Angular distribution of reflections in Laue diffraction. Acta Cryst.* A**47**, 352–373.

Garman, E. F. & Schneider, T. R. (1997). *Macromolecular cryocrystallography*. *J. Appl. Cryst.* **30**, 211–237.

Hajdu, J. & Johnson, L. N. (1993). *Biochemistry*, **29**, 1669–1675.

Helliwell, J. R. (1984). *Synchrotron X-radiation protein crystallography: instrumentation, methods and applications*. *Rep. Prog. Phys.* **47**, 1403–1497.

Helliwell, J. R. (1985). *Protein crystallography with synchrotron radiation*. *J. Mol. Struct.* **130**, 63–91.

Helliwell, J. R., Habash, J., Cruickshank, D. W. J., Harding, M. M., Greenhough, T. J., Campbell, J. W., Clifton, I. J., Elder, M., Machin, P. A., Papiz, M. Z. & Zurek, S. (1989). *The recording and analysis of synchrotron X-radiation Laue diffraction photographs. J. Appl. Cryst.* **22**, 483–497.

Helliwell, J. R. & Rentzepis, P. M. (1997). *Time Resolved Diffraction.* Oxford University Press.

Kalman, Z. H. (1979). *On the derivation of integrated reflected energy formulae. Acta Cryst.* A**35**, 634–641.

Moffat, K. (1989). *Time-resolved macromolecular crystallography*. *Annu. Rev. Biophys. Biophys. Chem.* **18**, 309–332.

Moffat, K. (1995). *Proc. Soc. Photo-Opt. Instrum. Eng.* **2521**, 182–187.

Moffat, K. (1997). *Laue diffraction*. *Methods Enzymol.* **277B**, 433–447.

Moffat, K. (1998). *Ultrafast time-resolved crystallography*. *Nature Struct. Biol.* **5**, 641–643.

Moffat, K., Bilderback, D., Schildkamp, W., Szebenyi, D. & Teng, T.-Y. (1989). In *Synchrotron Radiation in Structural Biology*, edited by R. M. Sweet and A. J. Woodhead, pp. 325–330. New York and London: Plenum Press.

Moffat, K., Szebenyi, D. & Bilderback, D. (1984). *X-ray Laue diffraction from protein crystals*. *Science*, **223**, 1423–1425.

Perman, B. (1999). PhD thesis, University of Chicago, USA.

Perman, B., Šrajer, V., Ren, Z., Teng, T.-Y., Pradervand, C., Ursby, T., Bourgeois, D., Schotte, F., Wulff, M., Kort, R., Hellingwerf, K. & Moffat, K. (1998). *Energy transduction on the nanosecond time scale: early structural events in a xanthopsin photocycle*. *Science*, **279**, 1946–1950.

Ren, Z., Bourgeois, D., Helliwell, J. R., Moffat, K., Šrajer, V. & Stoddard, B. L. (1999). *Laue crystallography: coming of age. J. Synchrotron Rad.* **6**, 891–917.

Ren, Z. & Moffat, K. (1994). *Laue crystallography for studying rapid reactions. J. Synchrotron Rad.* **1**, 78–82.

Ren, Z. & Moffat, K. (1995*a*). *Quantitative analysis of synchrotron Laue diffraction patterns in macromolecular crystallography. J. Appl. Cryst.* **28**, 461–481.

Ren, Z. & Moffat, K. (1995*b*). *Deconvolution of energy overlaps in Laue diffraction. J. Appl. Cryst.* **28**, 482–493.

Ren, Z., Ng, K., Borgstahl, G. E. O., Getzoff, E. D. & Moffat, K. (1996). *Quantitative analysis of time-resolved Laue diffraction patterns. J. Appl. Cryst.* **29**, 246–260.

Schlichting, I., Almo, S. C., Rapp, G., Wilson, K., Petratos, K., Lentfer, A., Wittinghofer, A., Kabsch, W., Pai, E. F., Petsko, G. A. & Goody, R. S. (1990). *Time-resolved X-ray crystallographic study of the conformational change in Ha-Ras p21 protein on GTP hydrolysis*. *Nature (London)*, **345**, 309–315.

Schlichting, I. & Goody, R. S. (1997). *Methods Enzymol.* **277B**, 467–490.

Šrajer, V., Teng, T.-Y., Ursby, T., Pradervand, C., Ren, Z., Adachi, S., Schildkamp, W., Bourgeois, D., Wulff, M. & Moffat, K. (1996). *Photolysis of the carbon monoxide complex of myoglobin: nanosecond time-resolved crystallography*. *Science*, **274**, 1726–1729.

Stoddard, B. L., Cohen, B. E., Brubaker, M., Mesecar, A. D. & Koshland, D. E. Jr (1998). *Millisecond Laue structures of an enzyme-product complex using photocaged substrate analogues*. *Nature Struct. Biol.* **5**, 891–897.

Wakatsuki, S. (1993). In *Data Collection and Processing*, edited by L. Sawyer, N. W. Isaacs & S. Bailey, pp. 71–79. DL/Sci/R34. Warrington: Daresbury Laboratory.

Wood, I. G., Thompson, P. & Mathewman, J. C. (1983). *A crystal structure refinement from Laue photographs taken with synchrotron radiation. Acta Cryst.* B**39**, 543–547.

Yang, X., Ren, Z. & Moffat, K. (1998). *Structure refinement against synchrotron Laue data: strategies for data collection and reduction. Acta Cryst.* D**54**, 367–377.